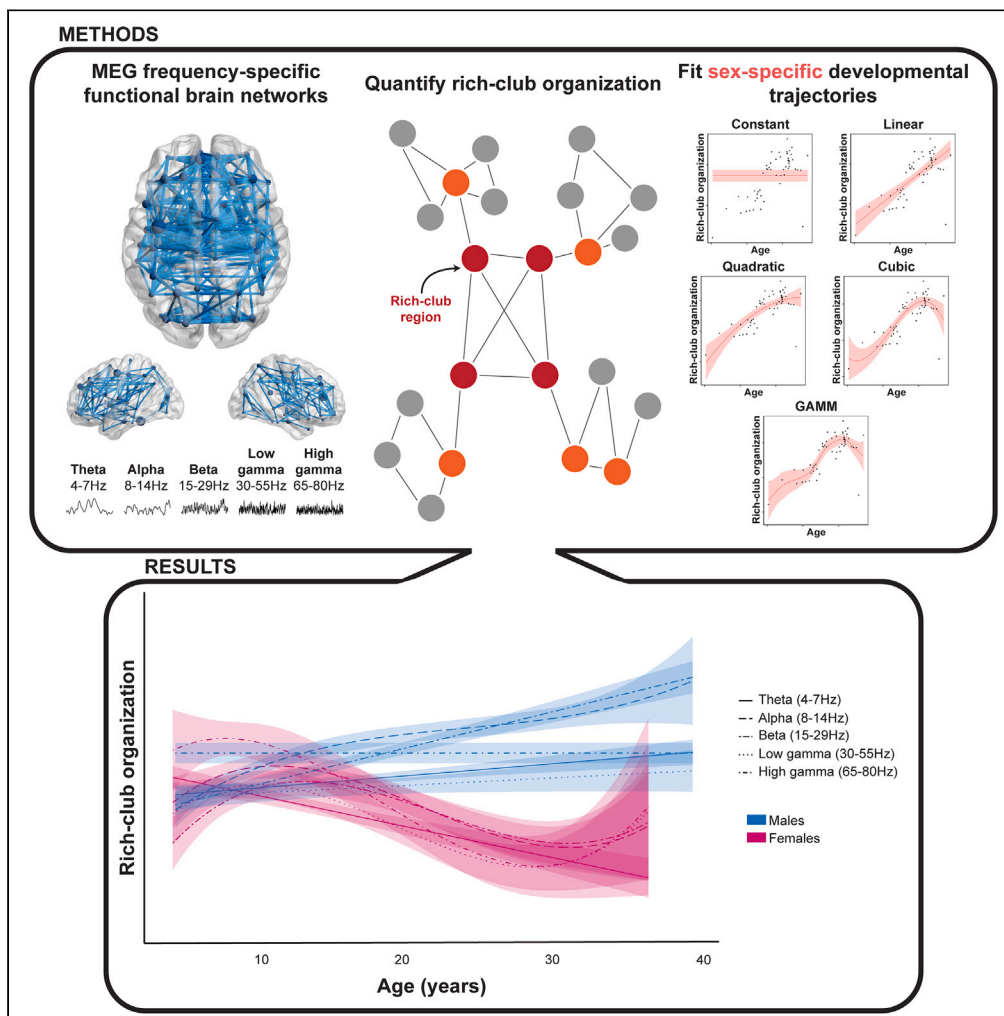## Article

Richer than we thought: neurophysiological methods reveal rich-club network development is frequency- and sex-dependent

Marlee M. Vandewouw, Elizabeth W. Pang, Meng-Chuan Lai, ..., Jason P. Lerch, Margot J. Taylor, Evdokia Anagnostou

mvandewouw@hollandbloorview.ca

Highlights

Development of the brain's rich-club organization differs between males and females

Developmental differences were observed in all five canonical frequency bands

Males show increased or no change in the rich-club organization with age

Females show increases through childhood, shifting to a decrease in adolescence

iScience

Article

Richer than we thought: neurophysiological methods reveal rich-club network development is frequency- and sex-dependent

Marlee M. Vandewouw,[1,2,3,17,*] Elizabeth W. Pang,[4,5] Meng-Chuan Lai,[4,6,7] Elizabeth Kelley,[8,9,10] Muhammad Ayub,[10] Jason P. Lerch,[4,11,12] Margot J. Taylor,[3,4,13,14,16] and Evdokia Anagnostou[1,4,15,16]

SUMMARY

A set of highly connected brain regions called the "rich-club" are vital in integrating information across the functional connectome. Although the literature has identified some changes in rich-club organization with age, little is known about potential sex-specific developmental trajectories, and neurophysiologically relevant frequency-dependent changes have not been established. Here we examine the frequency- and sex-dependent development of rich-club organization using magnetoencephalography in a large normative sample ($N = 383$) over a wide age span (4–39 years). We report strong divergence between males and females across alpha, beta, and gamma frequencies. While males show increased or no change in rich-club organization with age, females show a consistent, non-linear trajectory that increases through childhood, shifting direction in early adolescence. Using neurophysiological modalities for capturing complex inter-relations between oscillatory dynamics, age, and sex, we establish diverging, sex-specific developmental trajectories of the brain's core functional organization, critically important to our understanding of brain health and disease.

INTRODUCTION

The organization of the human brain can be described as a set of spatially distinct regions that are functionally integrated into a large-scale complex network, coined the connectome.[1] One key feature of the brain's functional connectome is the presence of network hubs—regions considerably more connected than others.[2,3] The brain is said to have "rich-club" organization when a small set of these hub brain regions tend to be more densely interconnected than connected to non-hub regions, a name originating from the observation that in social settings, wealthy individuals are very connected across society and highly connected to one another.[4] The regions in the rich-club, which usually include widely distributed areas such as the medial frontal and parietal cortices, the cingulate cortices, the inferior temporal cortices, and the insulae,[5,6] play a vital role in integrating information across the connectome, supporting a wide range of cognitive functions.[2] However, the connectivity density and widespread spatial distribution of the rich-club is costly in terms of anatomical wiring and metabolic requirements, making these regions particularly vulnerable to injury.[3,7,8] Thus, understanding the balance between information integration and vulnerability in the brain's rich-club organization could provide important insights into both health and disease.

Although the presence of a functional rich-club can be identified throughout development, the topography shifts from primary cortical regions in early life to a more distributed pattern across the association cortices by the end of childhood, reflecting the development of complex cognition over this period.[9–11] While there is consensus that the regions comprising the rich-club stabilize during adolescence, reports on the stability of the strength of the involved connections and importance to overall network function across the lifespan vary.[5,12–17] The functional connectivity of hub regions may even change non-linearly across the lifespan,[12,15] aligning with evidence of non-linear maturational trajectories of brain function.[18] Importantly, given that sex-related biological factors serve critical roles in normative brain development that result in sex-differential growth trajectories or age-dependent features,[19] it is surprising how little has been done to examine sex influences in functional rich-club development—only a few reports have noted differences in hubness but not the degree of rich-club organization.[12,20]

[1]Autism Research Centre, Bloorview Research Institute, Holland Bloorview Kids Rehabilitation Hospital, Toronto, ON M4G 1R8, Canada

[2]Institute of Biomedical Engineering, University of Toronto, Toronto, ON M5S 1A1, Canada

[3]Department of Diagnostic Imaging, Hospital for Sick Children, Toronto, ON M5G 1X8, Canada

[4]Program in Neurosciences and Mental Health, Research Institute, Hospital for Sick Children, Toronto, ON M5G 1X8, Canada

[5]Division of Neurology, Hospital for Sick Children, Toronto, ON M5G 1X8, Canada

[6]Campbell Family Mental Health Research Institute, Centre for Addiction and Mental Health, Toronto, ON M6J 1H4, Canada

[7]Department of Psychiatry, Temerty Faculty of Medicine, University of Toronto, Toronto, ON M5S 1A1, Canada

[8]Department of Psychology, Queen's University, Kingston, ON K7L 3N6 Canada

[9]Centre for Neuroscience Studies, Queen's University, Kingston, ON K7L 3N6 Canada

[10]Department of Psychiatry, Queen's University, Kingston, ON K7L 3N6 Canada

[11]Mouse Imaging Centre, Hospital for Sick Children, Toronto, ON M5G 1X8, Canada

[12]Wellcome Centre for Integrative Neuroimaging, FMRIB, Nuffield Department of Clinical Neurosciences, University of Oxford, Oxford OX3 9DU, UK

Continued

Table 1. Descriptive statistics of the participant demographics and corresponding statistics regarding each variable's relation to age

	Females	Males	Statistics
Datasets	191	288	–
Age range (years)	4–37	4–39	–
Age (years; mean ± std.)	14.46 ± 7.97	16.36 ± 8.72	Sex: $F_{(1, 477)} = 3.43$, p = 0.06
Rest type (Fixation: *Inscapes*)	164:27	247:41	Age: $F_{(1,475)} = 20.66$, p = 5.76×10^{-6} Sex: $F_{(1,475)} = 0.36$, p = 0.13 Age-by-sex: $F_{(1,475)} = 1.99$, p = 0.16
Head motion (mm; mean ± std.)	1.37 ± 1.13	1.30 ± 1.03	Age: $F_{(1,475)} = 155.32$, p = 1.64×10^{-30} Sex: $F_{(1,475)} = 0.93$, p = 0.34 Age-by-sex: $F_{(1,475)} = 2.11$, p = 0.15
Number of trials (mean ± std.)	21.71 ± 7.32	21.00 ± 6.88	Age: $F_{(1,475)} = 2.68$, p = 0.10 Sex: $F_{(1,475)} = 2.71$, p = 0.10 Age-by-sex: $F_{(1,475)} = 1.36$, p = 0.24
FSIQ range	77–140	76–149	–
FSIQ (mean ± std.)	114.49 ± 10.94	113.23 ± 1.89	Age: $F_{(1,410)} = 2.82$, p = 0.09 Sex: $F_{(1,410)} = 0.21$, p = 0.65 Age-by-sex: $F_{(1,410)} = 0.92$, p = 0.34

FSIQ: full scale intelligence quotient; std.: standard deviation.

Furthermore, all studies to date on the functional connectome's rich-club development have used functional magnetic resonance imaging (fMRI). Neurophysiological imaging modalities, such as magnetoencephalography (MEG) allow for the direct measurement of neuronal activity with high temporal resolution in milliseconds.[21] This high temporal resolution allows functional connectivity to be derived in a range of high-frequency bands which are known to support distinct cognitive functions[22–25] and to which fMRI is blind. Given that regions comprising the functional rich-club underlie a wide array of cognitive functions through information integration, examining the rich-club and the brain regions involved across different frequency bands will characterize their functional relevance. Finally, previous investigations into the development of the rich-club organization have employed statistical analysis on a group-averaged level,[5,12] aside from one study, that characterized rich-club organization on an individual level from infancy through adolescence.[20]

Here we extend the existing literature in three unique ways. We: 1) employ MEG to directly examine the rich oscillatory information available only with a neurophysiological modality; 2) quantify rich-club organization within individuals, allowing a consideration of the heterogeneity observed within the population; and 3) use a large single-site sample (383 typically developing individuals) encompassing a wide age span (4-39 years of age), several of whom underwent multiple scanning sessions, resulting in 479 data points. We demonstrate that the development of the functional rich-club is richer than we previously thought and shows both marked frequency- and sex-dependent developmental trajectories.

RESULTS

Participant demographics

The current retrospective study used resting-state MEG data which were acquired on 448 unique individuals (178 females, 270 males) between 4 and 39 years of age. Multiple resting-state acquisitions were collected on 114 participants (23 female, 91 male) and resting-state data were acquired longitudinally (>6 months) on 75 participants (24 female, 51 male), resulting in 665 datasets. Mixed-effects designs were chosen in the statistical analyses to use all available data. After excluding datasets for failing quality control (N = 75) and to ensure no between-sex differences in age nor head motion (N = 111), 479 datasets (191 female, 288 male) remained in our final sample.

Participant demographics are summarized in Table 1, along with statistical details regarding the main effects of age, sex, and age-by-sex interactions. Across the entire dataset, there was no significant difference in age between males and females ($F_{(1, 477)} = 3.43$, p = 0.06). With *Inscapes* being used to reduce head

[13]Department of Psychology, University of Toronto, Toronto, ON M5S 1A1, Canada

[14]Department of Medical Imaging, University of Toronto, Toronto, ON M5S 1A1, Canada

[15]Institute of Medical Science, University of Toronto, Toronto, ON M5S 1A1, Canada

[16]These authors contributed equally

[17]Lead contact

*Correspondence: mvandewouw@hollandbloorview.ca

Table 2. AIC values evaluating fit for each model investigating the effects of age on AURC in each frequency band for males and females

		Theta	Alpha	Beta	Low gamma	High gamma
Males	Constant	1204.99	1354.60	1412.64	1485.30	**1668.58**
	Linear	**1185.91**	1274.13	**1314.81**	**1484.11**	1670.10
	Quadratic	1187.62	1271.11	1316.66	1485.26	1671.07
	Cubic	1189.32	**1269.34**	1316.40	1487.08	1672.11
	GAMM	1187.91	1275.40	1316.81	1486.11	1672.10
Females	Constant	923.41	959.20	963.35	1041.63	1157.80
	Linear	**878.34**	936.88	962.47	1020.30	1118.10
	Quadratic	880.30	935.75	957.02	1022.29	1119.53
	Cubic	879.83	**928.71**	**950.09**	**1015.53**	**1115.87**
	GAMM	880.34	936.49	958.77	1022.30	1120.10

AIC: Akaike Information Criteria; GAMM: general additive mixed model.
Optimal values are bolded.

motion in children, there was a significant effect of age on rest type ($F_{(1,475)} = 20.66$, $p = 5.76 \times 10^{-6}$); however, there was no main effect of sex ($F_{(1,475)} = 0.36$, $p = 0.13$) nor an age-by-sex interaction ($F_{(1,475)} = 1.99$, $p = 0.16$). There was a relation between age and mean head motion ($F_{(1,475)} = 155.32$, $p = 1.64 \times 10^{-30}$), with head motion decreasing with increasing age, and hence head motion was regressed from the amplitude envelope timeseries (see STAR Methods: MEG preprocessing); there was no main effect of sex or age-by-sex interaction on mean head motion (sex: $F_{(1,475)} = 0.93$, $p = 0.34$, age-by-sex: $F_{(1,475)} = 2.11$, $p = 0.15$). Excess trials were removed for some participants to ensure no significant main effects of age ($F_{(1,475)} = 2.68$, $p = 0.20$), sex ($F_{(1,475)} = 2.71$, $p = 0.10$), or age-by-sex interaction ($F_{(1,475)} = 1.36$, $p = 0.24$) on the number of trials. Full-scale intelligence quotient (FSIQ) was collected for 414 datasets, and there was no effect of age ($F_{(1,410)} = 2.82$, $p = 0.09$), sex ($F_{(1,410)} = 0.21$, $p = 0.65$), nor age-by-sex interaction ($F_{(1,410)} = 0.92$, $p = 0.34$)

Area under the rich-club curve

Resting-state functional connectivity networks were constructed for each participant and each of the canonical frequency bands (theta: 4-7Hz, alpha: 8-14Hz, beta: 15-29Hz, low gamma: 30-55Hz, and high gamma: 65-80Hz). Rich-club coefficient curves were constructed for each network and statistical significance was assessed. The area under the curve of significant rich-club coefficients (AURC) was used to quantify each network's rich-club organization.

Five age models (constant, linear, quadratic, and cubic polynomials, and a general additive mixed model (GAMM)) were fit to the AURC data for each frequency band for males and females, and Akaike Information Criteria (AIC) values, used to compare the quality of the models, are presented in Table 2. In the theta and alpha bands, the linear and cubic models, respectively, were optimal in both males and females. However, modeling age as linear was optimal for the remaining bands (beta, low gamma, and high gamma) in the males, yet cubic for the females.

The sex-specific developmental trajectories are visualized separately for each frequency band in Figure 1 and presented in a single plot in Figure S1. The corresponding features of interest (with 95% confidence intervals) for the optimal models for each frequency band and sex are shown in Table 3. The parameter estimates and statistical details corresponding to the optimal models for the males and females are presented in Table S1.

In theta, the linear effect of age on AURC was significant within each sex (Table 3 and Figure 1A). in females, rich-club organization decreased with age, while the opposite pattern was observed in the males, with the sexes showing a statistically significant difference in slope ($p < 1.00 \times 10^{-4}$).

In the alpha band, the cubic effect of age was significant in the females, while only the quadratic term was significant in the males (Table 3). This is reflected when observing the within-group developmental
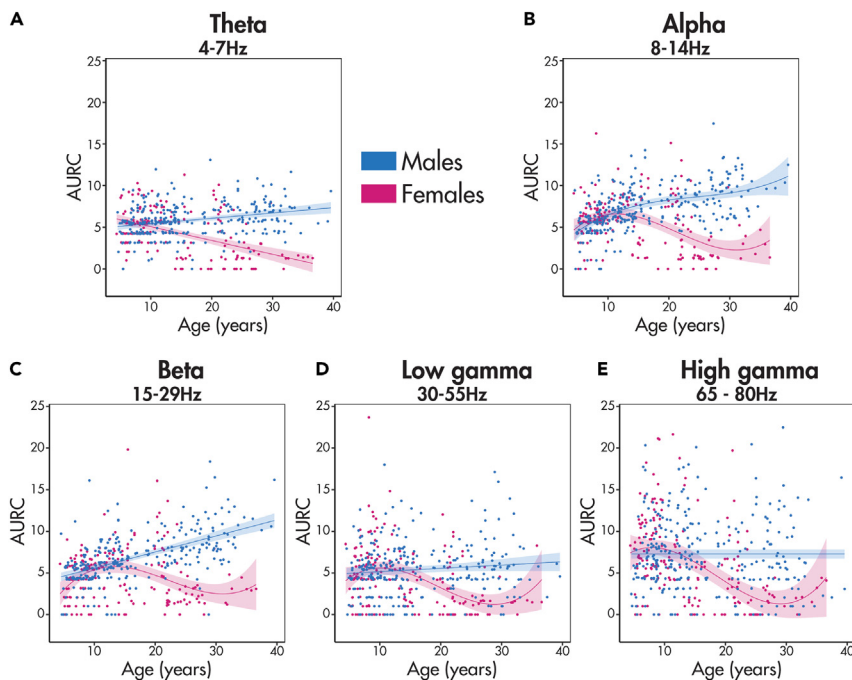
Figure 1. Developmental trajectories of the rich-club organization (area under the rich-club curve (AURC)) in the males (blue) and females (pink) for each frequency band
(A and E) (A: theta, B: alpha, C: beta, D: low gamma, E: high gamma). The fitted trajectory is presented as a solid line with a shaded 95% confidence interval, and data points for each participant are scatter plotted.

trajectories and their corresponding features (Figure 1B). All three features of interest were stable in the subsampling procedure in the females: rich-club organization increased until late childhood before beginning to decrease, followed by an inflection point in early adulthood and a local minimum in adulthood. In the males, however, the local maximum and minimum were only present in less than 1% of the subsamples, respectively, and were highly variable, indicating an unstable cubic trajectory.

In the beta frequency band, a significant cubic effect of age on rich-club organization was observed in the females, while the males showed a significant linear positive relation (Table 3 and Figure 1C). In the beta frequency band, the female cubic trajectory reached its features of interest at a slightly later age compared to in alpha.

In low gamma, the females again exhibited a significant cubic relation between age and rich-club organization, while the males had no significant change in the rich-club organization with age, although the subsampling results for slope did indicate a weak positive relation (Table 3 and Figure 1D). The cubic relation in the females reached its features of interest earlier in life compared to the other frequency bands (alpha and beta). Similarly, in high gamma, the females exhibited a significant cubic relation between age and rich-club organization, reaching most of its features of interest even earlier than in low gamma, while the males exhibited no relation (Table 3 and Figure 1E). Global efficiency was also examined by sex to enable a comparison to fMRI literature; rich-club organization primarily increased with age in the lower frequency bands, with little-to-no changes with age in the higher frequency bands, and minimal sex differences (Table S2 and Figure S2).

Rich-club regions

We also investigated which brain regions were part of the rich club and how these evolved with age, frequency, and sex. The regions belonging to the rich-club were extracted for each participant and frequency band, and the age models were fit with the binomial distribution given the binary nature of rich-club membership. Optimal fits between age and the probability of being a rich-club region were identified by AIC values for each brain region and frequency band in males and females and are presented in Figure S3.

Table 3. For each frequency band and sex, optimal fits describing the relation between age and rich-club organization are indicated with the corresponding features of interest and their 95% confidence intervals (indicated in square brackets) and the percentage of subsamples for which the feature was present (indicated in round brackets)

		Theta	Alpha	Beta	Low gamma	High gamma
Males	Optimal fit	Linear	Cubic	Linear	Linear	Constant
	Slope	0.06 [0.04, 0.08]	–	0.19 [0.17, 0.22]	0.04 [0.01, 0.07]	–
	Maximum	–	30.56 [20.36, 38.46] (1%)	–	–	–
	Inflection point	–	24.51 [21.74, 30.84] (0.4%)	–	–	–
	Minimum	–	11.06 [4.75, 33.53] (95%)	–	–	–
Females	Optimal fit	Linear	Cubic	Cubic	Cubic	Cubic
	Slope	−0.16 [-0.19, −0.14]	–	–	–	–
	Maximum	–	11.06 [10.24, 12.65] (100%)	13.48 [12.49, 14.47] (100%)	9.98 [7.76, 11.32] (100%)	7.87 [5.07, 10.05] (89%)
	Inflection point	–	21.60 [20.05, 23.48] (100%)	22.61 [21.15, 24.70] (99%)	19.46 [17.99, 20.96] (100%)	18.22 [14.98, 19.84] (100%)
	Minimum	–	31.57 [29.03, 34.60] (98%)	31.61 [29.53, 34.43] (98%)	28.94 [26.88, 31.55] (100%)	29.22 [28.02, 30.78] (100%)

To demonstrate the changes, from the optimal fits the probability of regions belonging to the rich-club were predicted and binarized at 5, 18, and 30 years of age for each sex in each frequency band and presented in Figure 2.

Brain regions with statistically significant (p_{corr}<0.05) changes in rich-club membership with age are presented in Figure 3: primarily, females showed significant changes with age, and these changes were predominantly linear (Figure 3A and Table S3). Some non-linear (quadratic and cubic, Figures 3B and 3C; Tables S4 and S5) changes were observed in females. Linear effects were observed in males (Figure 3D) in the alpha and beta frequency bands.

Specifically, in the theta band, the females demonstrated widespread decreases in the probability of being a rich-club region throughout the brain; subsampling revealed slope means and 95% confidence intervals that were consistently negative. The males showed no significant changes with age in the theta band. A negative relation between age and rich-club membership in the alpha band was observed in the left lingual gyrus in the females and left putamen in the males. Quadratic changes in rich-club membership with age in females were observed in the beta band, with the developmental trajectories following a U-shaped curve in the right orbital part of the middle frontal gyrus and left rectus, amygdala, caudate, and pallidum. All regions reached their minimum in late adolescence (17.39-19.01 years). A cubic change in membership with age was observed in the females in the beta band in the right cuneus: membership increased until 12.54 years (95% CI: [11.57, 13.41]), before decreasing with an inflection point at 19.62 years (95% CI: [18.18, 20.95]) and reaching a minimum at 26.17 years (95% CI: [24.21, 27.73]). Conversely, the males showed a decrease in rich-club membership with age in the bilateral orbitofrontal cortices, left rectus and anterior cingulate gyrus, and right putamen. Decreases with age in rich-club membership were found in low gamma in regions including the left orbitofrontal cortex, left insula, right hippocampal, parahippocampal, lingual, and fusiform gyri, bilateral thalami, and bilateral temporal regions in the females; no changes with age were observed in the males. Finally, no changes in rich-club membership with age were observed in either sex in high gamma.

DISCUSSION

Using MEG to investigate the wealth of information available in both temporal and oscillatory domains, combined with analytic methods that account for sex-specificity, individual variability, and a large sample size encompassing children and adults, we demonstrate, for the first time, sex- and frequency-dependent development in the rich-club network in humans. We anchored our findings to the existing fMRI literature via a supplemental analysis of global efficiency: our data were concordant with prior fMRI studies, which reported primarily increases with age and small sex differences in children and adolescents.[20] Importantly, it is only when we use neurophysiological recordings that striking sex and developmental differences emerge.
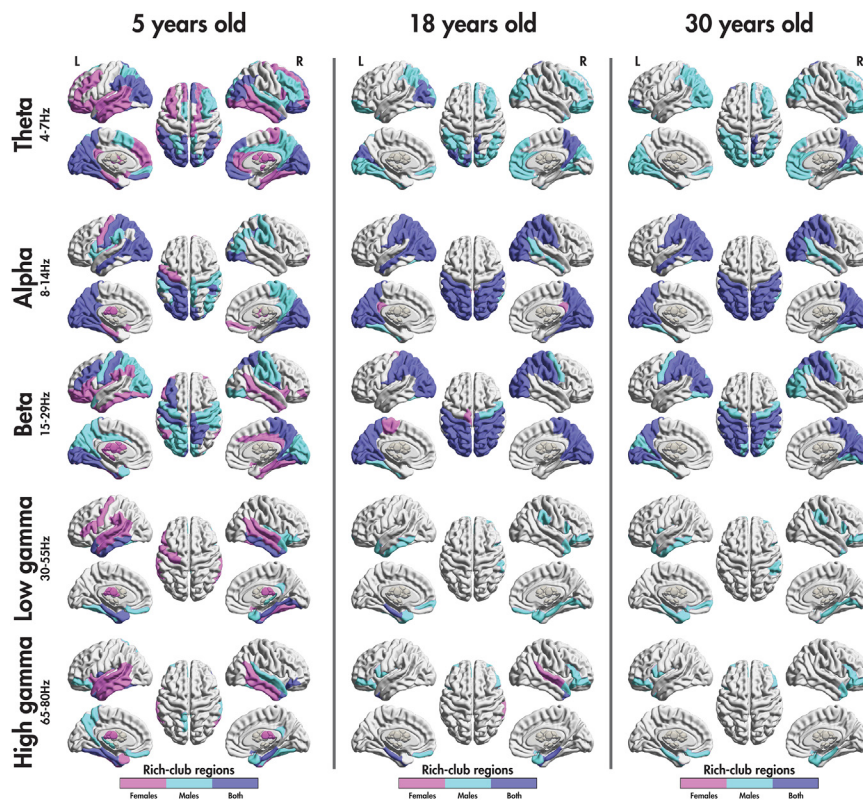
Figure 2. Brain regions predicted to belong to the female (pink), male (blue), and both female and male (purple) rich-clubs at 5, 18, and 30 years of age

Across alpha, beta, and gamma frequency bands, a remarkable dissociation was observed where males showed a significant positive linear effect of age in beta, no effect of age on rich-club membership in gamma (low or high), and high variability across individuals in alpha. In contrast, across alpha, beta, and both gamma frequency bands, females showed a cubic effect of age with a maximum in early adolescence, an inflection point in young adulthood with a minimum around age 30 years. Further, these effects were highly homogeneous in females with close to all subsamples fitting the model.

In males, our findings suggest that, with increasing age, there is increasing engagement of the rich-club network only in the beta band. While recent research has identified broader roles for beta oscillations in working memory and executive control,[26] it is well established that these oscillations are key in coordinating sensory perceptions with motor functions,[27] especially visuospatial processing which is known to be superior in males, on average (e.g.,[28,29]). Our functional connectome findings are in line with work showing sex differences in the human structural connectome such that brain regions that facilitated these skills were preferentially connected in males.[30]

In females, engagement of the rich-club network in all frequency bands followed non-linear trajectories, increasing through childhood, shifting direction in adolescence until it reached a minimum in the early adult years, followed by a subsequent increase. These data suggest that by the early teen years, females' functional brain organization has diverged substantially from that of males, with females engaging more distributed, less rich-club-centric networks, across all frequency bands. This finding converges with the evidence that the brain structural connectome in females tends to organize in a way that better facilitates signal exchange across hemispheres and between distributed brain regions[30] and fits with the observation that females show higher verbal ability on average,[31] as language function is subsumed by a distributed network.[32] Furthermore, this non-linear development in neurophysiological network organization in females also corresponds with the known non-linear developmental trajectories in cerebral blood flow in females, from childhood to early adulthood, which also shows remarkable sex-differences from mid-adolescence.[33]
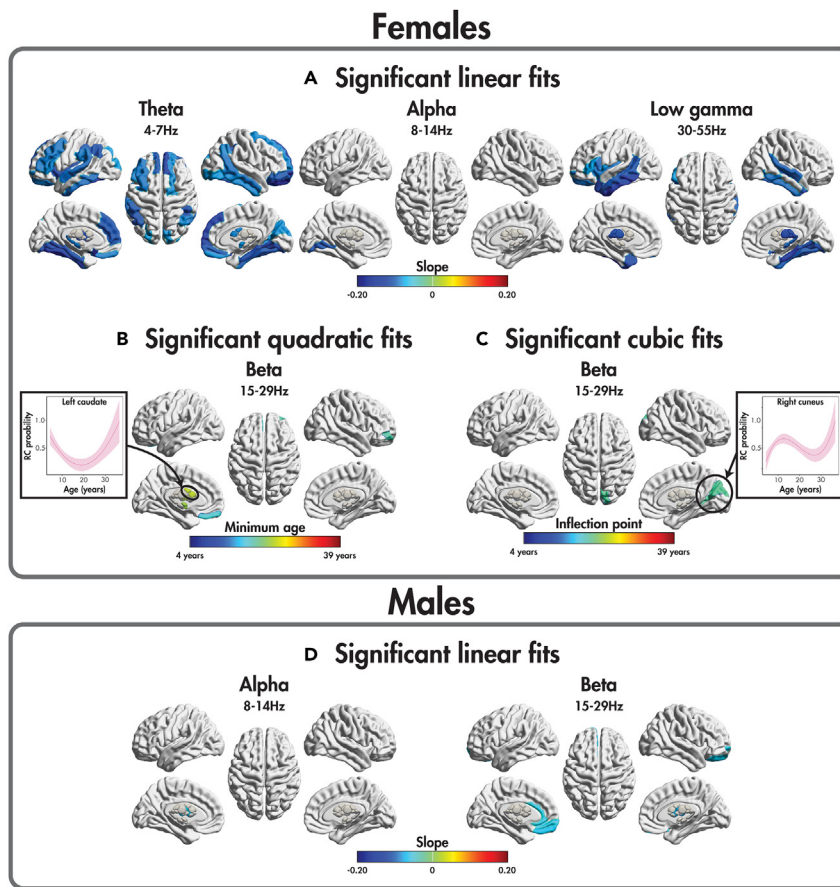
Figure 3. Regions showing significant effects of age on rich-club membership
Regions showing significant linear, quadratic, and cubic effects of age on rich-club membership for females (A – C) and males (D). The fitted trajectory for two example regions is presented as a solid line with a shaded 95% confidence interval.

Our current work significantly extends the increasing evidence of normative brain developmental differences by sex and sex-related biological factors,[19,34] and the critical importance of accounting for such sex-differential distributions and trajectories to understand the basis of neurocognitive differences associated with sex and mechanisms of neuropsychiatric disorders with unbalanced male-female ratios[35,36] (for reviews, see[37–39]). Enhanced rich-club network, as seen in our male cohort, may have both advantages and disadvantages developmentally. It is thought that the rich-club architecture evolved to maximize performance by more efficiently using metabolic resources, shortening relay and processing times, and building in redundancy to enhance the robustness and prevent breakdown.[3] However, this design may render the rich-club network vulnerable to pathology.[40] A meta-analysis[41] identified a list of brain disorders with lesions significantly more likely to be in rich-club hubs. One example at the top of the list is schizophrenia which more often affects males, especially in young adulthood.[42] Interestingly, frontotemporal dementia which affects males and females equally in late midlife (45-65 years)[43] and Alzheimer's dementia, which preferentially affects senior females (>65 years),[44] were both high on this list, although these conditions typically present beyond the age range examined in this study. Finally, our finding that, with age, males increasingly engaged the rich-club network only in the beta band also links to the potential relevance to diseases involving pathological beta oscillatory synchronization, such as Parkinson disease.[45]

On the other hand, a distributed network also has advantages and disadvantages. Females on average show greater resilience to adversity, most likely supported by stronger social networks,[46] better social cognition skills such as emotional processing,[47] face processing,[48] and empathy,[49] as well as better verbal ability.[31] These functions all are subsumed by distributed brain networks (e.g.,[32,50,51]). However,

a disadvantage of utilizing a distributed network may include heightened vulnerability toward disorders involving multiple brain regions or extensive cortical-subcortical interactions, such as depression[52] and post-traumatic stress disorder,[53] both of which are significantly more likely to occur in females.[54-57]

This divergence in rich-club network engagement occurs between sexes in the pubertal years, reaching minima in the middle of the reproductive years, suggesting these differences emerge in part due to biological mechanisms. For example, sex hormones are known to have a role in shaping brain structure, particularly during sensitive developmental periods including puberty,[58] when there are marked alterations in sex hormones and significant changes in cognition[59] (see,[60] for a review). Unlike males, where the levels of sex hormones remain relatively stable across adulthood, females show cycling patterns during reproductive years. There is fMRI evidence that monthly hormonal cycles affect cognitive function[61,62] and widespread patterns of brain connectivity[63] in females. Furthermore, gendered experiences that are differentially embodied by female vs. male individuals across development may further shape the observed sex-differential network topology,[64] mediated via biological mechanisms.[65] Notably, our finding that nearly all the female subsamples fit the non-linear models shows a more similar rich-club organization within females compared to that within males, corresponding to the emerging fMRI findings of higher intra-female similarity in the brain resting-state network topography compared to that in males.[66] More importantly, it demonstrates that we can measure very stable features of the female functional brain network.

The striking divergence of rich-club trajectories as youth transition into adolescence in our cohort may not have been predicted by previous fMRI results.[12,15] However, given that fMRI studies use the hemodynamic response to indirectly measure brain physiology, and the known effects of sex hormones on the vascular system,[67] this modality may be confounded by the variability in hormone-induced vascular changes affecting the hemodynamic signal, and therefore introduce instability into BOLD-based measurement of network topology. This highlights the need for non-BOLD-based neuroimaging modalities to detect age and sex effects.

Our results highlight the critical importance of considering sex-specific developmental trajectories in brain physiology and network topology and understanding their relation to vulnerability and resilience in brain development, cognition, and brain-based disorders and diseases.[38,68-72] Future studies should consider the measurement of sex hormones, as well as gender-based experiential indices, to better capture developmental mechanisms and distinguish effects of cycling hormones during estrous cycles from the more stable effects of sex on the sex-specific rich-club organization we observed in this study.

In summary, we report striking age-related sex differences in the brain's rich-club network which only emerge as we investigate across oscillatory frequency bands. We submit that the richness of the brain's dynamic properties in the time, space, and oscillatory domains can only be captured with the use of neurophysiological modalities. It is only when we apply these high spatial-temporal resolution methods to the examination of brain oscillations and their role in brain network communications that we will gain a full picture of sex (and subsequently, gender) differences in brain function necessary to understand health and disease across the lifespan.

Limitations of the study

A limitation of our study is the smaller sample of females in the older age range compared to the males, which could bias our trajectory shapes; while we have addressed this limitation by ensuring the features of interest occurring in adulthood are stable across subsamples in the females (present in at least 98% of subsamples), future work should validate our trajectories with a more balanced sample distribution. Furthermore, there is an increasing awareness of the importance of both reliability and reproducibility in developmental neuroimaging analyses.[73,74] While we have a large sample size (particularly for developmental MEG studies), reliability is also a key determinant in statistical power, placing an upper bound on the maximum identifiable effect size and requiring extremely large samples to achieve required effect sizes.[74] The chosen MEG connectivity metric and network thresholding has been identified as having high test-retest reliability for a set of global graph measures that are related to the rich-club organization in comparison to other popular techniques.[75] Thus, while we have not measured reliability directly in this study,

this reported reliability coupled with our sample size suggests that the current study has sufficient statistical power. While high reliability is a requirement for high validity,[74,76] establishing the reproducibility of our results is still necessary. While we attempted to address this issue using our subsampling procedure, future work should use an independently collected sample to validate our findings, as no such dataset was publicly available at the time of publication.

STAR★METHODS

Detailed methods are provided in the online version of this paper and include the following:

- KEY RESOURCES TABLE
- RESOURCE AVAILABILITY
  - Lead contact
  - Materials availability
  - Data and code availability
- EXPERIMENTAL MODEL AND SUBJECT DETAILS
- METHOD DETAILS
  - MEG acquisition
  - MEG processing
  - Rich-club
- QUANTIFICATION AND STATISTICAL ANALYSIS
  - Participant demographics
  - AURC
  - Rich-club regions

SUPPLEMENTAL INFORMATION

Supplemental information can be found online at https://doi.org/10.1016/j.isci.2023.106384.

AUTHOR CONTRIBUTIONS

Conceptualization: M.M.V., M.J.T., and E.A.; methodology: M.M.V.; software: M.M.V.; formal analysis: M.M.V.; resources: E.K., M.A., J.P.L., M.J.T., and E.A.; writing – original draft: M.M.V., E.W.*Preschool and E.A.; writing – review & editing: M.M.V., E.W.P., M.C.L., E.K., M.A., J.P.L., M.J.T., and E.A.; visualization: M.M.V; supervision: M.J.T. and E.A.; funding acquisition: J.P.L., M.J.T., and E.A.

DECLARATION OF INTERESTS

E. Anagnostou has served as a consultant to Roche, Quadrant Therapeutics, ONO, and Impel Pharmaceuticals, holds a patent for the device, "Anxiety Meter," and has received in kind support from AMO pharma and CRA, royalties from APPI and Springer, and editorial honoraria from Wiley. The remaining authors have reported no financial interests or potential conflicts of interest.

INCLUSIONS AND DIVERSITY

We support inclusive, diverse, and equitable conduct of research.

REFERENCES

1. Bullmore, E., and Sporns, O. (2009). Complex brain networks: graph theoretical analysis of structural and functional systems. Nat. Rev. Neurosci. *10*, 186–198. https://doi.org/10.1038/nrn2575.

2. van den Heuvel, M.P., and Sporns, O. (2013). Network hubs in the human brain. Trends Cogn. Sci. *17*, 683–696. https://doi.org/10.1016/j.tics.2013.09.012.

3. Collin, G., Sporns, O., Mandl, R.C.W., and Van Den Heuvel, M.P. (2014). Structural and functional aspects relating to cost and benefit of rich club organization in the human cerebral cortex. Cereb. Cortex *24*, 2258–2267. https://doi.org/10.1093/cercor/bht064.

4. Karolis, V.R., Froudist-Walsh, S., Brittain, P.J., Kroll, J., Ball, G., Edwards, A.D., Dell'Acqua, F., Williams, S.C., Murray, R.M., and Nosarti, C. (2016). Reinforcement of the brain's rich-club architecture following early neurodevelopmental disruption caused by very preterm birth. Cereb. Cortex *26*, 1322–1335. https://doi.org/10.1093/cercor/bhv305.

5. Grayson, D.S., Ray, S., Carpenter, S., Iyer, S., Dias, T.G.C., Stevens, C., Nigg, J.T., and Fair, D.A. (2014). Structural and functional rich club organization of the brain in children and adults. PLoS One *9*, e88297. https://doi.org/10.1371/journal.pone.0088297.

6. van den Heuvel, M.P., and Sporns, O. (2011). Rich-club organization of the human connectome. J. Neurosci. *31*, 15775–15786. https://doi.org/10.1523/jneurosci.3539-11.2011.

7. Bullmore, E., and Sporns, O. (2012). The economy of brain network organization. Nat. Rev. Neurosci. *13*, 336–349. https://doi.org/10.1038/nrn3214.

8. van den Heuvel, M.P., Kahn, R.S., Goñi, J., and Sporns, O. (2012). High-cost, high-capacity backbone for global brain communication. Proc. Natl. Acad. Sci. USA *109*, 11372–11377. https://doi.org/10.1073/PNAS.1203593109/SUPPL_FILE/PNAS.201203593SI.PDF.

9. Oldham, S., and Fornito, A. (2019). The development of brain network hubs. Dev. Cogn. Neurosci. *36*, 100607. https://doi.org/10.1016/j.dcn.2018.12.005.

10. Dong, H.M., Margulies, D.S., Zuo, X.N., and Holmes, A.J. (2021). Shifting gradients of macroscale cortical organization mark the transition from childhood to adolescence. Proc. Natl. Acad. Sci. USA *118*, e2024448118. https://doi.org/10.1073/PNAS.2024448118/SUPPL_FILE/PNAS.2024448118.SD02.TXT.

11. Zuo, X.N., He, Y., Betzel, R.F., Colcombe, S., Sporns, O., and Milham, M.P. (2017). Human connectomics across the life span. Trends Cogn. Sci. *21*, 32–45. https://doi.org/10.1016/J.TICS.2016.10.005.

12. Cao, M., Wang, J.H., Dai, Z.J., Cao, X.Y., Jiang, L.L., Fan, F.M., Song, X.W., Xia, M.R., Shu, N., Dong, Q., et al. (2014). Topological organization of the human brain functional connectome across the lifespan. Dev. Cogn. Neurosci. *7*, 76–93. https://doi.org/10.1016/j.dcn.2013.11.004.

13. Zuo, X.N., Ehmke, R., Mennes, M., Imperati, D., Castellanos, F.X., Sporns, O., and Milham, M.P. (2012). Network centrality in the human functional connectome. Cereb. Cortex *22*, 1862–1875. https://doi.org/10.1093/cercor/bhr269.

14. Hwang, K., Hallquist, M.N., and Luna, B. (2013). The development of hub architecture in the human functional brain network. Cereb. Cortex *23*, 2380–2393. https://doi.org/10.1093/cercor/bhs227.

15. Wu, K., Taki, Y., Sato, K., Hashizume, H., Sassa, Y., Takeuchi, H., Thyreau, B., He, Y., Evans, A.C., Li, X., et al. (2013). Topological organization of functional brain networks in healthy children: differences in relation to age, sex, and intelligence. PLoS One *8*, e55347. https://doi.org/10.1371/journal.pone.0055347.

16. Uddin, L.Q., Supekar, K.S., Ryali, S., and Menon, V. (2011). Dynamic reconfiguration of structural and functional connectivity across core neurocognitive brain networks with development. J. Neurosci. *31*, 18578–18589. https://doi.org/10.1523/JNEUROSCI.4465-11.2011.

17. Betzel, R.F., Byrge, L., He, Y., Goñi, J., Zuo, X.N., and Sporns, O. (2014). Changes in structural and functional connectivity among resting-state networks across the human lifespan. Neuroimage *102 Pt 2*, 345–357. https://doi.org/10.1016/J.NEUROIMAGE.2014.07.067.

18. Hunt, B.A.E., Wong, S.M., Vandewouw, M.M., Brookes, M.J., Dunkley, B.T., and Taylor, M.J. (2019). Spatial and spectral trajectories in typical neurodevelopment from childhood to middle age. Netw. Neurosci. *3*, 497–520. https://doi.org/10.1162/netn_a_00077.

19. Kaczkurkin, A.N., Raznahan, A., and Satterthwaite, T.D. (2019). Sex differences in the developing brain: insights from multimodal neuroimaging. Neuropsychopharmacology *44*, 71–85. https://doi.org/10.1038/S41386-018-0111-Z.

20. Gozdas, E., Holland, S.K., and Altaye, M.; CMIND Authorship Consortium (2019). Developmental changes in functional brain networks from birth through adolescence. Hum. Brain Mapp. *40*, 1434–1444. https://doi.org/10.1002/hbm.24457.

21. Brookes, M.J., Hale, J.R., Zumer, J.M., Stevenson, C.M., Francis, S.T., Barnes, G.R., Owen, J.P., Morris, P.G., and Nagarajan, S.S. (2011). Measuring functional connectivity using MEG: Methodology and comparison with fcMRI. Neuroimage *56*, 1082–1104. https://doi.org/10.1016/j.neuroimage.2011.02.054.

22. Solomon, E.A., Kragel, J.E., Sperling, M.R., Sharan, A., Worrell, G., Kucewicz, M., Inman, C.S., Lega, B., Davis, K.A., Stein, J.M., et al. (2017). Widespread theta synchrony and high-frequency desynchronization underlies enhanced cognition. Nat. Commun. *8*, 1704. https://doi.org/10.1038/s41467-017-01763-2.

23. Foxe, J.J., and Snyder, A.C. (2011). The role of alpha-band brain oscillations in selective attention. Front. Psychol. *2*, 154.

24. Sherman, M.A., Lee, S., Law, R., Haegens, S., Thorn, C.A., Hämäläinen, M.S., Moore, C.I., and Jones, S.R. (2016). Neural mechanisms of transient neocortical beta rhythms: converging evidence from humans, computational modeling, monkeys, and mice. Proc. Natl. Acad. Sci. USA *113*, E4885–E4894. https://doi.org/10.1073/pnas.1604135113.

25. Fries, P. (2009). Neuronal gamma-band synchronization as a fundamental process in cortical computation. Annu. Rev. Neurosci. *32*, 209–224. https://doi.org/10.1146/annurev.neuro.051508.135603.

26. Schmidt, R., Herrojo Ruiz, M., Kilavik, B.E., Lundqvist, M., Starr, P.A., and Aron, A.R. (2019). Beta oscillations in working memory, executive control of movement and thought, and sensorimotor function. J. Neurosci. *39*, 8231–8238. https://doi.org/10.1523/JNEUROSCI.1163-19.2019.

27. Salenius, S., and Hari, R. (2003). Synchronous cortical oscillatory activity during motor action. Curr. Opin. Neurobiol. *13*, 678–684. https://doi.org/10.1016/j.conb.2003.10.008.

28. Linn, M.C., and Petersen, A.C. (1985). Emergence and characterization of sex differences in spatial ability: a meta-analysis. Child Dev. *56*, 1479–1498.

29. Maeda, Y., and Yoon, S.Y. (2013). A meta-analysis on gender differences in mental rotation ability measured by the purdue spatial visualization tests: visualization of rotations (PSVT:R). Educ. Psychol. Rev. *25*, 69–94. https://doi.org/10.1007/s10648-012-9215-x.

30. Ingalhikar, M., Smith, A., Parker, D., Satterthwaite, T.D., Elliott, M.A., Ruparel, K., Hakonarson, H., Gur, R.E., Gur, R.C., and Verma, R. (2014). Sex differences in the structural connectome of the human brain. Proc. Natl. Acad. Sci. USA *111*, 823–828. https://doi.org/10.1073/pnas.1316909110.

31. Hyde, J.S., and Linn, M.C. (1988). Gender differences in verbal ability: a meta-analysis. Psychol. Bull. *104*, 53–69. https://doi.org/10.1037/0033-2909.104.1.53.

32. Hickok, G. (2009). The functional neuroanatomy of language. Phys. Life Rev. *6*, 121–143. https://doi.org/10.1016/j.plrev.2009.06.001.

33. Satterthwaite, T.D., Shinohara, R.T., Wolf, D.H., Hopson, R.D., Elliott, M.A., Vandekar, S.N., Ruparel, K., Calkins, M.E., Roalf, D.R., Gennatas, E.D., et al. (2014). Impact of

puberty on the evolution of cerebral perfusion during adolescence. Proc. Natl. Acad. Sci. USA *111*, 8643–8648. https://doi.org/10.1073/PNAS.1400178111/-/DCSUPPLEMENTAL/PNAS.201400178SI.PDF.

34. Bethlehem, R.A.I., Seidlitz, J., White, S.R., Vogel, J.W., Anderson, K.M., Adamson, C., Adler, S., Alexopoulos, G.S., Anagnostou, E., Areces-Gonzalez, A., et al. (2022). Brain charts for the human lifespan. Nature *604*, 525–533. https://doi.org/10.1038/S41586-022-04554-Y.

35. White, J., Tannenbaum, C., Klinge, I., Schiebinger, L., and Clayton, J. (2021). The integration of sex and gender considerations into biomedical research: lessons from international funding agencies. J. Clin. Endocrinol. Metab. *106*, 3034–3048. https://doi.org/10.1210/CLINEM/DGAB434.

36. Joel, D., and McCarthy, M.M. (2017). Incorporating sex as a biological variable in neuropsychiatric research: where are we now and where should we Be? Neuropsychopharmacology *42*, 379–385. https://doi.org/10.1038/NPP.2016.79.

37. Cahill, L. (2006). Why sex matters for neuroscience. Nat. Rev. Neurosci. *7*, 477–484. https://doi.org/10.1038/nrn1909.

38. Loke, H., Harley, V., and Lee, J. (2015). Biological factors underlying sex differences in neurological disorders. Int. J. Biochem. Cell Biol. *65*, 139–150. https://doi.org/10.1016/j.biocel.2015.05.024.

39. Pinares-Garcia, P., Stratikopoulos, M., Zagato, A., Loke, H., and Lee, J. (2018). Sex: a significant risk factor for neurodevelopmental and neurodegenerative disorders. Brain Sci. *8*, 154. https://doi.org/10.3390/brainsci8080154.

40. Griffa, A., and Van den Heuvel, M.P. (2018). Rich-club neurocircuitry: function, evolution, and vulnerability. Dialogues Clin. Neurosci. *20*, 121–132.

41. Crossley, N.A., Mechelli, A., Scott, J., Carletti, F., Fox, P.T., Mcguire, P., and Bullmore, E.T. (2014). The hubs of the human connectome are generally implicated in the anatomy of brain disorders. Brain *137*, 2382–2395. https://doi.org/10.1093/brain/awu132.

42. Aleman, A., Kahn, R.S., and Selten, J.-P. (2003). Sex differences in the risk of schizophrenia: evidence from meta-analysis. Arch. Gen. Psychiatry *60*, 565–571. https://doi.org/10.1001/archpsyc.60.6.565.

43. Onyike, C.U., and Diehl-Schmid, J. (2013). The epidemiology of frontotemporal dementia. Int. Rev. Psychiatry *25*, 130–137. https://doi.org/10.3109/09540261.2013.776523.

44. Mielke, M.M., Vemuri, P., and Rocca, W.A. (2014). Clinical epidemiology of Alzheimer's disease: assessing sex and gender differences. Clin. Epidemiol. *6*, 37–48. https://doi.org/10.2147/CLEP.S37929.

45. Hammond, C., Bergman, H., and Brown, P. (2007). Pathological synchronization in Parkinson's disease: networks, models and treatments. Trends Neurosci. *30*, 357–364. https://doi.org/10.1016/j.tins.2007.05.004.

46. Cohen, S., and Janicki-Deverts, D. (2009). Can we improve our physical health by altering our social networks? Perspect. Psychol. Sci. *4*, 375–378. https://doi.org/10.1111/j.1745-6924.2009.01141.x.

47. Kret, M.E., and De Gelder, B. (2012). A review on sex differences in processing emotional signals. Neuropsychologia *50*, 1211–1221. https://doi.org/10.1016/j.neuropsychologia.2011.12.022.

48. Herlitz, A., and Lovén, J. (2013). Sex differences and the own-gender bias in face recognition: a meta-analytic review. Vis. cogn. *21*, 1306–1336. https://doi.org/10.1080/13506285.2013.823140.

49. Christov-Moore, L., Simpson, E.A., Coudé, G., Grigaityte, K., Iacoboni, M., and Ferrari, P.F. (2014). Empathy: gender effects in brain and behavior. Neurosci. Biobehav. Rev. *46 Pt 4*, 604–627. https://doi.org/10.1016/j.neubiorev.2014.09.001.

50. Adolphs, R. (2009). The social brain: neural basis of social knowledge. Annu. Rev. Psychol. *60*, 693–716. https://doi.org/10.1146/annurev.psych.60.110707.163514.

51. Proverbio, A.M. (2021). Sex differences in the social brain and in social cognition. J. Neurosci. Res. https://doi.org/10.1002/jnr.24787.

52. Pandya, M., Altinay, M., Malone, D.A., and Anand, A. (2012). Where in the brain is depression? Curr. Psychiatry Rep. *14*, 634–642. https://doi.org/10.1007/s11920-012-0322-7.

53. Shin, L.M., Rauch, S.L., and Pitman, R.K. (2006). Amygdala, medial prefrontal cortex, and hippocampal function in PTSD. Ann. N. Y. Acad. Sci. *1071*, 67–79. https://doi.org/10.1196/annals.1364.007.

54. Cyranowski, J.M., Frank, E., Young, E., and Shear, M.K. (2000). Adolescent onset of the gender difference in lifetime rates of major depression: a theoretical model. Arch. Gen. Psychiatry *57*, 21–27. https://doi.org/10.1001/archpsyc.57.1.21.

55. Kessler, R.C., and Bromet, E.J. (2013). The epidemiology of depression across cultures. Annu. Rev. Public Health *34*, 119–138. https://doi.org/10.1146/annurev-publhealth-031912-114409.

56. Breslau, N., Davis, G.C., Andreski, P., Peterson, E.L., and Schultz, L.R. (1997). Sex differences in posttraumatic stress disorder. Arch. Gen. Psychiatry *54*, 1044–1048. https://doi.org/10.1001/archpsyc.1997.01830230082012.

57. Lewis, S.J., Arseneault, L., Caspi, A., Fisher, H.L., Matthews, T., Moffitt, T.E., Odgers, C.L., Stahl, D., Teng, J.Y., and Danese, A. (2019). The epidemiology of trauma and post-traumatic stress disorder in a representative cohort of young people in England and Wales. Lancet Psychiatr. *6*, 247–256. https://doi.org/10.1016/S2215-0366(19)30031-8.

58. Rehbein, E., Hornung, J., Sundström Poromaa, I., and Derntl, B. (2021). Shaping of the female human brain by sex hormones: a review. Neuroendocrinology *111*, 183–206. https://doi.org/10.1159/000507083.

59. Beltz, A.M., and Moser, J.S. (2020). Ovarian hormones: a long overlooked but critical contributor to cognitive brain structures and function. Ann. N. Y. Acad. Sci. *1464*, 156–180. https://doi.org/10.1111/nyas.14255.

60. Hornung, J., Lewis, C.A., and Derntl, B. (2020). Sex hormones and human brain function. In Handbook of Clinical Neurology, pp. 195–207. https://doi.org/10.1016/B978-0-444-64123-6.00014-X.

61. Albert, K., Pruessner, J., and Newhouse, P. (2015). Estradiol levels modulate brain activity and negative responses to psychosocial stress across the menstrual cycle. Psychoneuroendocrinology *59*, 14–24. https://doi.org/10.1016/j.psyneuen.2015.04.022.

62. Syan, S.K., Minuzzi, L., Costescu, D., Smith, M., Allega, O.R., Coote, M., Hall, G.B.C., and Frey, B.N. (2017). Influence of endogenous estradiol, progesterone, allopregnanolone, and dehydroepiandrosterone sulfate on brain resting state functional connectivity across the menstrual cycle. Fertil. Steril. *107*, 1246–1255.e4. https://doi.org/10.1016/j.fertnstert.2017.03.021.

63. Pritschet, L., Santander, T., Taylor, C.M., Layher, E., Yu, S., Miller, M.B., Grafton, S.T., and Jacobs, E.G. (2020). Functional reorganization of brain networks across the human menstrual cycle. Neuroimage *220*, 117091. https://doi.org/10.1016/J.NEUROIMAGE.2020.117091.

64. Fine, C., Dupré, J., and Joel, D. (2017). Sex-linked behavior: evolution, stability, and variability. Trends Cogn. Sci. *21*, 666–673. https://doi.org/10.1016/J.TICS.2017.06.012.

65. van Anders, S.M., Steiger, J., and Goldey, K.L. (2015). Effects of gendered behavior on testosterone in women and men. Proc. Natl. Acad. Sci. USA *112*, 13805–13810. https://doi.org/10.1073/PNAS.1509591112.

66. Li, L., Cui, Z., and Wang, L. (2022). A more female-characterized resting-state brain: graph similarity analyses of sex influence on the human brain intrinsic functional network. Brain Topogr. *35*, 341–351. https://doi.org/10.1007/S10548-022-00900-5.

67. Krause, D.N., Duckles, S.P., and Pelligrino, D.A. (2006). Influence of sex steroid hormones on cerebrovascular function. J. Appl. Physiol. *101*, 1252–1261. https://doi.org/10.1152/JAPPLPHYSIOL.01095.2005/ASSET/IMAGES/LARGE/ZDG0100668430005.JPEG.

68. Hägg, S., and Jylhävä, J. (2021). Sex differences in biological aging with a focus

on human studies. Elife *10*, e63425. https://doi.org/10.7554/eLife.63425.

69. Hausmann, M. (2021). Sex/gender differences in brain activity - it's time for a biopsychosocial approach to cognitive neuroscience. Cogn. Neurosci. *12*, 178–179. https://doi.org/10.1080/17588928.2020.1853087.

70. Slotnick, S.D. (2021). Sex differences in the brain. Cogn. Neurosci. *12*, 103–105. https://doi.org/10.1080/17588928.2021.1957808.

71. Hodes, G.E., and Epperson, C.N. (2019). Sex differences in vulnerability and resilience to stress across the life span. Biol. Psychiatry *86*, 421–432. https://doi.org/10.1016/j.biopsych.2019.04.028.

72. Bale, T.L., and Epperson, C.N. (2017). Sex as a biological variable: who, what, when, why, and how. Neuropsychopharmacology *42*, 386–396. https://doi.org/10.1038/npp.2016.215.

73. Klapwijk, E.T., van den Bos, W., Tamnes, C.K., Raschle, N.M., and Mills, K.L. (2021). Opportunities for increased reproducibility and replicability of developmental neuroimaging. Dev. Cogn. Neurosci. *47*, 100902. https://doi.org/10.1016/J.DCN.2020.100902.

74. Zuo, X.-N., Xu, T., Milham, M.P., Zuo, X.-N., Xu, T., and Milham, M.P. (2019). Harnessing reliability for neuroscience research. Nat. Hum. Behav. *3*, 768–771. https://doi.org/10.1038/S41562-019-0655-X.

75. Pourmotabbed, H., de Jongh Curry, A.L., Clarke, D.F., Tyler-Kabara, E.C., and Babajani-Feremi, A. (2022). Reproducibility of graph measures derived from resting-state MEG functional connectivity metrics in sensor and source spaces. Hum. Brain Mapp. *43*, 1342–1357. https://doi.org/10.1002/HBM.25726.

76. Kraemer, H.C. (2014). The reliability of clinical diagnoses: state of the art. Annu. Rev. Clin. Psychol. *10*, 111–130. https://doi.org/10.1146/ANNUREV-CLINPSY-032813-153739.

77. Oostenveld, R., Fries, P., Maris, E., and Schoffelen, J.M. (2011). FieldTrip: open source software for advanced analysis of MEG, EEG, and invasive electrophysiological data. Comput. Intell. Neurosci. *2011*, 156869. https://doi.org/10.1155/2011/156869.

78. R Core Team (2022). R: A Language and Environment for Statistical Computing.

79. Bates, D., Mächler, M., Bolker, B., and Walker, S. (2015). Fitting linear mixed-effects models using lme4. J. Stat. Softw. *67*, 1–48. https://doi.org/10.18637/JSS.V067.I01.

80. Wood, S.N., and Scheipl, F. (2020). gamm4: generalized Additive Mixed Models using 'mgcv'and 'lme4'.

81. May, T., Adesina, I., McGillivray, J., and Rinehart, N.J. (2019). Sex differences in neurodevelopmental disorders. Curr. Opin. Neurol. *32*, 622–626. https://doi.org/10.1097/WCO.0000000000000714.

82. Vanderwal, T., Kelly, C., Eilbott, J., Mayes, L.C., and Castellanos, F.X. (2015). Inscapes: a movie paradigm to improve compliance in functional magnetic resonance imaging. Neuroimage *122*, 222–232. https://doi.org/10.1016/j.neuroimage.2015.07.069.

83. Vandewouw, M.M., Dunkley, B.T., Lerch, J.P., Anagnostou, E., and Taylor, M.J. (2021). Characterizing Inscapes and resting-state in MEG: effects in typical and atypical development. Neuroimage *225*, 117524. https://doi.org/10.1016/j.neuroimage.2020.117524.

84. Wechsler, D. (1999). Wechsler Abbreviated Scales of Intelligence (The Psychological Corporation).

85. Wechsler, D. (2003). Weschler Intelligence Scale for Children, 4th ed. (The Psychological Corporation).

86. Wechsler, D. (2014). Wechsler Intelligence Scale for Children, 5th ed. (Pearson).

87. Wechsler, D. (2012). The Wechsler Preschool and Primary Scale of Intelligence, 4th ed. (The Psychological Corporation).

88. The Mathworks Inc. (2018). MATLAB. www.mathworks.com/products/matlab.

89. Pang, E.W. (2011). Practical aspects of running developmental studies in the MEG. Brain Topogr. *24*, 253–260. https://doi.org/10.1007/s10548-011-0175-0.

90. Van Veen, B.D., Van Drongelen, W., Yuchtman, M., and Suzuki, A. (1997). Localization of brain electrical activity via linearly constrained minimum variance spatial filtering. IEEE Trans. Biomed. Eng. *44*, 867–880. https://doi.org/10.1109/10.623056.

91. Tzourio-Mazoyer, N., Landeau, B., Papathanassiou, D., Crivello, F., Etard, O., Delcroix, N., Mazoyer, B., and Joliot, M. (2002). Automated anatomical labeling of activations in SPM using a macroscopic anatomical parcellation of the MNI MRI single-subject brain. Neuroimage *15*, 273–289. https://doi.org/10.1006/nimg.2001.0978.

92. Nolte, G. (2003). The magnetic lead field theorem in the quasi-static approximation and its use for magnetoenchephalography forward calculation in realistic volume conductors. Phys. Med. Biol. *48*, 3637–3652. https://doi.org/10.1088/0031-9155/48/22/002.

93. Colclough, G.L., Brookes, M.J., Smith, S.M., and Woolrich, M.W. (2015). A symmetric multivariate leakage correction for MEG connectomes. Neuroimage *117*, 439–448. https://doi.org/10.1016/j.neuroimage.2015.03.071.

94. Messaritaki, E., Koelewijn, L., Dima, D.C., Williams, G.M., Perry, G., and Singh, K.D. (2017). Assessment and elimination of the effects of head movement on MEG resting-state measures of oscillatory brain activity. Neuroimage *159*, 302–324. https://doi.org/10.1016/j.neuroimage.2017.07.038.

95. Luppi, A.I., and Stamatakis, E.A. (2021). Combining network topology and information theory to construct representative brain networks. Netw. Neurosci. *5*, 96–124. https://doi.org/10.1162/netn_a_00170.

96. Sporns, O. (2010). Networks of the Brain, 1st ed. (The MIT Press).

97. Dimitriadis, S.I., Antonakakis, M., Simos, P., Fletcher, J.M., and Papanicolaou, A.C. (2017). Data-driven topological filtering based on orthogonal minimal spanning trees: application to multigroup magnetoencephalography resting-state connectivity. Brain Connect. *7*, 661–670. https://doi.org/10.1089/brain.2017.0512.

98. Wang, J., Wang, X., Xia, M., Liao, X., Evans, A., and He, Y. (2015). GRETNA: a graph theoretical network analysis toolbox for imaging connectomics. Front. Hum. Neurosci. *9*, 386. https://doi.org/10.3389/fnhum.2015.00386.

99. Maslov, S., and Sneppen, K. (2002). Specificity and stability in topology of protein networks. Science *296*, 910–913. https://doi.org/10.1126/science.1065103.

100. Sporns, O., and Zwi, J.D. (2004). The small world of the cerebral cortex. Neuroinformatics *2*, 145–162. https://doi.org/10.1385/NI:2:2:145.

101. Hastie, T., and Tibshirani, R. (1986). Generalized additive models. Stat. Sci. *1*, 297–310. https://doi.org/10.1214/ss/1177013604.

102. Zuur, A.F., Ieno, E.N., Walker, N.J., Saveliev, A.A., and Smith, G.M. (2009). Mixed Effects Models and Extensions in Ecology with R (Springer).

103. Efron, B. (1983). Estimating the error rate of a prediction rule: improvement on cross-validation. J. Am. Stat. Assoc. *78*, 316–331. https://doi.org/10.1080/01621459.1983.10477973.

STAR★METHODS

KEY RESOURCES TABLE

REAGENT or RESOURCE	SOURCE	IDENTIFIER
Deposited data		
Raw data and participant information	Brain-CODE (Ontario Brain Institute)	ARK ID 70798/d7qv7rj6b98w66v7m3
Software and algorithms		
Custom code	This study	https://doi.org/10.5281/zenodo.7503841
FieldTrip	Oostenveld et al., 2011[77]	Git commit 4c12371
MATLAB	MathWorks	R2021a
R	R Core Team[78]	Version 4.1.1
lme4	Bates et al., 2015[79]	Version 1.1–27.1
gamm4	Wood et al., 2020[80]	Version 0.2–6

RESOURCE AVAILABILITY

Lead contact

Further information and requests for resources should be directed to and will be fulfilled by the lead contact, Marlee Vandewouw (mvandewouw@hollandbloorview.ca).

Materials availability

There are no newly generated materials to report.

Data and code availability

- Data drawn from the Province of Ontario Neurodevelopmental Disorders network are available through the Ontario Brain Institute's BRAIN-CODE (https://www.braincode.ca/) in a controlled data release. Data drawn from the studies supported by Canadian Institutes of Health Research grants will be shared by the lead contact upon reasonable request.

- Original code has been deposited at Zenodo and is publicly available as of the date of publication. DOIs are listed in the key resources table.

- Any additional information required to reanalyze the data reported in this paper is available from the lead contact upon request.

EXPERIMENTAL MODEL AND SUBJECT DETAILS

Resting-state MEG data were acquired on 448 unique individuals (178 females, 270 males) between 4–39 years of age for multiple studies at the Hospital for Sick Children between 2011 and 2020: the Province of Ontario Neurodevelopmental Disorders (POND) network, an Integrated Discovery System co-directed by E. Anagnostou and J.P. Lerch and funded by the Ontario Brain Institute, and studies supported by Canadian Institutes of Health Research (CIHR) grants awarded to M.J. Taylor. The POND study is comprised of children and adolescents who have been diagnosed with neurodevelopmental disorders along side those who are typically developing; similarly, many of the CIHR grants were for studies of autism spectrum disorder. Given that neurodevelopmental disorders are diagnosed in males at a higher rate than females,[81] the typically developing controls from both sets of cohorts were recruited to match this imbalance, which is reflected in the sex distribution of the current retrospective study. The Hospital for Sick Children's Research Ethics Board approved all protocols. Due to some individuals participating in several studies, multiple resting-state acquisitions (e.g., fixation-cross and *Inscapes*,[82,83] see next section) were collected during the same scanning session on 114 participants (23 female, 91 male) and resting-state data were acquired longitudinally (>6 months) on 75 participants (24 female, 51 male), resulting in 665 datasets. Full-scale intelligence quotient (FSIQ) was collected on the participants using age-appropriate scales.[84–87] Participants were excluded from the current analyses if there was a history of preterm birth,

neurodevelopmental, psychiatric, or neurological disorders, or the presence of contraindications for MEG and/or MRI. Informed consent was obtained from all participants who were old enough to do so; otherwise, informed assent was obtained from the child and informed consent was obtained from their guardian.

METHOD DETAILS

MEG acquisition

Resting-state MEG data were acquired on a 151-channel CTF system (CTF-MEG International Services LP, Coquitlam, Canada; 600Hz sampling rate, 3rd order spatial gradient, 0–150Hz antialiasing recording band-pass) within a magnetically shielded room. Five-minutes of either fixation-cross or *Inscapes*[82,83] eyes-open resting-state was obtained for each participant. We have previously shown that differences in MEG connectivity between fixation-cross resting-state and *Inscapes* are localized to regions in the visual network (which have not been reported to be involved in the rich-club). In the fixation-cross paradigm, a grey cross was centered within a grey circle on a black background, which was back-projected onto a screen positioned ∼70cm from the participant's eyes; the participants were instructed to fixate on the cross. In the *Inscapes* paradigm, the first five minutes of the naturalistic movie was back-projected onto the screen, accompanied by the piano score being played over the speakers in the MEG suite. Fiducial coils were used to continuously track head motion during the MEG acquisition.

A T1-weighted MRI image was obtained after replacing the fiducial coils with radio-opaque markers to allow for the generation of subject-specific head models. The images were acquired on either a 3T MAGNETOM Siemens (Siemens Healthcare AG, Erlangen, Germany) Trio scanner with a 12-channel head coil or Prisma^{fit} scanner with a 20-channel head and neck coil due to a scanner upgrade (Trio: TR/TE/TI = 2300/2.96/900ms, FA = 9°, FOV = 240 × 256mm, # slices = 192, resolution = 1mm isotropic, scan time = 5:03min; Prisma^{fit}: TR/TE/TI = 1870/3.14/945ms, FA = 9°, FOV = 240 × 256mm, # slices = 192, resolution = 0.8mm isotropic, scan time = 5:10min).

MEG processing

Data were epoched into 10s segments and preprocessed using the FieldTrip[77] MATLAB[88] toolbox. Preprocessing consisted of bandpass filtering (1–150Hz, 4th order two-pass Butterworth), notch filtering (60 and 120Hz, discrete Fourier transform), and removal of artefacts from eye movements and cardiac signal. Epochs with sensor signals exceeding 2000fT or with head motion exceeding 10mm[89] from the median head position were excluded from the data. Participants were required to have at least one minute of resting-state data remaining, and excess epochs were randomly excluded from some participants to ensure no main effect of age on the number of trials remaining and no effects of the mean head motion across the remaining trials.

The linearly constrained minimum variance (LCMV) beamformer[90] was used to estimate the timeseries of the 90 cortical and subcortical regions of the Automated Anatomical Labeling (AAL) atlas[91] in source space. The anatomical MRIs were co-registered to the sensor space MEG data via the fiducials, and a single-shell subject-specific head model was constructed.[92] The anatomical MRIs were nonlinearly normalized to MNI space, and the MNI coordinates of the AAL centroids were subsequently unwarped into the subject-space of the head models. The head models were used to compute the lead fields generated by unit current dipoles in three dimensions at each centroid. Covariance matrices were computed across all selected epochs within a 1–150Hz broadband window with 5% Tikhonov regularization. The LCMV beamformer constructs weights for the spatial filters that constrains the filters to pass neural activity from the 90 sources, using the lead fields, while minimizing activity stemming from other regions, using the covariance matrices.[90] The beamformer is applied to the sensor data, producing timeseries of the cortical activity at each source; the timeseries are subsequently normalized by the estimated noise to mitigate spatial non-uniformity in the distribution of noise.

The timeseries for each brain region were mean-centered and filtered into five frequency bands (theta: 4–7Hz, alpha: 8–14Hz, beta: 15–29Hz, low gamma: 30–55Hz, and high gamma: 65–80Hz) using the Hamming window to design a two-pass finite impulse response filter. The filtered data were corrected for source leakage using a symmetric orthogonalization technique,[93] the amplitude envelopes were computed using the Hilbert transform. Given that this is the first study examining the development of rich-club organization using MEG, the resulting timeseries were down-sampled to 1Hz to enable comparison of our results with the existing fMRI literature.

Due to the inherent relation between head motion and the participants ages, a more stringent head motion correction procedure was chosen over simply including head motion as a covariate in the statistical analyses.[94] For each sample, the positions of the three fiducial coils were used to extract the displacement of the coils from its position at the start of the recording. The three displacement measurements were also used to calculate a measure of "instantaneous motion" by computing the change in displacement between consecutive samples. Like the amplitude envelope timeseries, the six head motion timeseries were epoched into 10s segments, down-sampled to 1Hz, and z-scored. These head motion timeseries were regressed from the amplitude envelope timeseries.

A connectivity network was computed for each participant and frequency band using Pearson correlations between the motion-regressed amplitude envelope timeseries for pairs of brain regions, resulting in a fully dense network with all edges having nonzero connectivity values. Thresholding fully dense networks has been shown to increase biological plausibility and eliminate spurious connection weights.[95,96] A thresholding technique using orthogonal minimum spanning trees (OMST[97]) was chosen. Minimal spanning trees (MSTs) are the subset of a network's edges that connects all nodes of the network without cycles while minimizing its cost, or the sum of all edge weights. OMST thresholding iteratively identifies and removes MSTs from the original network, aggregating the MSTs and calculating a measure of global cost efficiency until its value is optimized, returning the set of MSTs as the thresholded network. OMST thresholding has been validated on MEG data[97] and shown to produce networks with a biologically plausible amount of sparseness while sustaining its representativeness.[95]

Rich-club

The weighted rich-club coefficient measures the presence of rich-club organization in a participant's weighted network; that is, it measures whether highly connected nodes are more strongly interconnected to one another than what would be expected by chance.[6] Formally, with degree defined as the number of connections extending from a node, the weighted rich-club coefficient for degree k ($\Phi^w(k)$) is calculated by extracting the subnetwork containing only the nodes having a degree exceeding k; this subnetwork consists of n edges. Then, $\Phi^w(k)$ is calculated by taking the ratio between the sum of the n connection weights of the subnetwork and the sum of the n largest weights in the original network. For each k, the regions belonging to the network's rich-club are defined as the regions whose degree (number of edges extending from the region) exceeds k. This calculation was performed for participants' frequency-dependent network over the range of k. To assess whether a coefficient was greater than what would be expected by chance, the observed rich-club coefficient was normalized ($\Phi^w_{norm}(k)$) by the mean weighted rich-club coefficient of 1000 random networks with the same degree distribution.[98–100] A statistical p-value was assigned to each $\Phi^w_{norm}(k)$ using the null distribution, and the p-values were corrected over the range of k. Rich-club organization was deemed to exist if $\Phi^w_{norm}(k)$ was statistically significant ($p_{corr} < 0.05$) over a range of k. The area under the curve of significant rich-club coefficients (area under the rich-club curve, or AURC) was used to quantify each network's rich-club organization, with a value of zero indicating no rich-club organization and increasingly positive values indicating increased rich-club organization. Any brain region whose degree exceeded the minimum k for which the network demonstrated rich-club organization was said to belong to the rich-club. Finally, to allow comparison with previous fMRI studies,[20] we also computed global efficiency for each participant.

QUANTIFICATION AND STATISTICAL ANALYSIS

Participant demographics

Linear mixed effects models were used to test for differences in age between males and females across the entire dataset using the R (version 4.1.1[78]) package *lme4* (version 1.1–27.1[79]). Given the relation between head motion, and thus the number of epochs used in the analysis, and age, linear mixed effects models were used to test for main effects of age, sex, and age-by-sex interactions on these variables. A linear mixed effect model was also used to test for main effects of age, sex, and age-by-sex interactions on the rest type (fixation-cross and *Inscapes*), modeling the response variable with a binomial distribution.

AURC

First, the effects of age on AURC were examined in each frequency band for males and females using the R (version 4.1.1[78]) package *gamm4* (version 0.2–6[80]). To characterize the developmental trajectories in each sex, linear and non-linear mixed effects models were fitted; mixed effects designs were chosen to use all

available data, including the multiple resting-state acquisitions in the same scanning session and the longitudinal data. Age was modeled as (1) constant, (2) linear, (3) quadratic, and (4) cubic:

$$(1)\ \textbf{Constant} : AURC \sim (1|Subject)$$

$$(2)\ \textbf{Linear} : AURC \sim Age + (1|Subject)$$

$$(3)\ \textbf{Quadratic} : AURC \sim Age + Age^2 + (1|Subject)$$

$$(4)\ \textbf{Cubic} : AURC \sim Age + Age^2 + Age^3 + (1|Subject)$$

Additionally, a general additive mixed model (GAMM;[101]) was used to model age as a (5) non-parametric smooth function, which, unlike linear mixed models, requires no *a priori* assumptions on the specific polynomial form of the data:

$$(5)\ \textbf{GAMM} : AURC \sim s(Age) + (1|Subject)$$

In this model, age is modeled as a smooth term defined by the smooth function *s*(), which was set to thin plate penalized smooth spline. For each frequency band, all five models were fit to the AURC data for males and females, and the quality of the models was compared using the Akaike Information Criteria (AIC), chosen to enable comparison of GAMMs and non-GAMMs. Since AIC values from models fit with the Restricted Maximum Likelihood (REML) estimation cannot be compared if the models contain different factors,[102] the models were fit with Maximum Likelihood (ML) estimation for AIC calculation. Furthermore, to ensure that the likelihood estimation was consistent across the models, all were fit using the *gamm4* package. Once the optimal model was selected for each frequency band for the males and females, REML estimation was used to extract the parameter estimates and statistical details; significance was held at p <0.05. Note that models were fit independently to both sexes rather than in a single model with interactions to ease interpretation given the observation that males and females demonstrated different optimal fits in most frequency bands (see Table 2).

For frequencies showing significant effects of age on AURC, features of interest characteristic of each type of model were examined in each sex. For linear fits, the feature of interest is the slope – the rate of change of AURC with age. For the quadratic fit, the feature of interest is the vertex – the age at which the curve reaches a maximum or minimum. For the cubic fit, the features of interest are local minimums and maximums, along with what is called an "inflection point" – the age at which the curve transitions from concave upward, where the slope is increasing, to concave downward, where the slope is decreasing (or vice versa). Subsampling was used to calculate a distribution of each feature of interest for each sex. For each iteration, 63.2% of the datasets for the males and 63.2% of the datasets for the females were extracted, the optimal model was fit for each set, and the feature of interest was calculated.[103] This was performed for 10,000 iterations, generating a distribution of the feature for each sex from which the means and 95% confidence intervals could be determined. Note that the presence of the listed features for GAMMs is dependent on its estimated degrees of freedom, and only features that occur within the examined age range (4–39 years) were extracted, thus not all features may be present in each iteration. Hence, the percentage of iterations for which the feature is present is reported as a measure of stability along with narrow confidence intervals. A feature of interest common to both males and females was determined to be significantly different between the groups if >95% of the iterations showed a difference in the same direction (e.g., 95% of the iterations showed an increase in the feature in females compared to males, or males compared to females).

Rich-club regions
An identical procedure was employed to investigate how regions belonging to the rich-club changed with age and sex. Models were fit with the binomial distribution given the binary nature of rich-club membership, and thus the probability of a region being in the rich-club was evaluated across age; p-values were Bonferroni corrected across brain regions to control for multiple comparisons.